Fuel 341 (2023) 127706

Contents lists available at ScienceDirect

Fuel

journal homepage: www.elsevier.com/locate/fuel

Release of phosphorus from thermal conversion of phosphorus-rich biomass chars – Evidence for carbothermic reduction of phosphates

Emil O. Lidman Olsson [a,b,c], Daniel Schmid [d], Oskar Karlström [e], Kasper Enemark-Rasmussen [f], Henrik Leion [g], Songgeng Li [b,h], Peter Glarborg [a], Kim Dam-Johansen [a], Hao Wu [a,*]

[a] Department of Chemical and Biochemical Engineering, Technical University of Denmark, Søltofts Plads, Building 229, 2800 Kgs, Lyngby, Denmark
[b] Sino-Danish College, University of Chinese Academy of Sciences, Eastern Yanqihu campus, 380 Huaibeizhuang, Huairou district, Beijing 101400, China
[c] Sino-Danish Center for Education and Research, Eastern Yanqihu campus, 380 Huaibeizhuang, Huairou district, Beijing 101400, China
[d] Group of Inorganic Chemistry, Johan Gadolin Process Chemistry Centre, Åbo Akademi University, Henrikinkatu 2, 20500 Turku, Finland
[e] Industrial Engineering and Management, Department of Mechanical and Materials Engineering, University of Turku, Turun Yliopisto, 20014 Turku, Finland
[f] Department of Chemistry, Technical University of Denmark, Kemitorvet Building 207, 2800 Kgs. Lyngby, Denmark
[g] Department of Chemistry and Chemical Engineering, Chalmers University of Technology, Kemigården 4, 412 96 Gothenburg, Sweden
[h] Institute of Process Engineering, University of Chinese Academy of Sciences, 1 North 2nd Street, Zhongguancun, Haidian District, Beijing 100190, China

ARTICLE INFO

Keywords:
Phosphorus
Potassium
Biomass
Release
Thermal conversion
Carbothermic reduction

ABSTRACT

Biomass can be used to generate heat, power, or biofuels in thermal conversion processes such as combustion, gasification and pyrolysis. However, some types of biomass contain high levels of phosphorus, which can be released to the gas phase and cause operational or environmental problems. The mechanism(s) responsible for phosphorus release has not been convincingly established. Understanding the high-temperature phosphorus chemistry is also important in order to enable efficient recovery of phosphorus in residues from thermal conversion of biomass. In this work, the release of phosphorus from wheat bran char and sunflower seed char in different gas environments (100 % N_2, 1–20 % O_2, and 10 % CO_2) and temperatures (900–1100 °C) was studied. The chars were converted in a horizontal tube reactor and characterized using ICP-OES, XRD, SEM-EDS, and ^{31}P NMR. The release of ash-forming elements was determined using ICP-OES analysis of the char and sample residues, whereas the release of carbon was determined using CO and CO_2 gas analysis. In both chars, phosphorus was present primarily together with potassium and magnesium, mainly as pyrophosphates in the wheat bran char, and largely as orthophosphates in the sunflower seed char. For wheat bran char, the release of phosphorus increased from 27 % at 900 °C to 71 % at 1100 °C in N_2, whereas the release was at least 20 % lower in the oxidizing atmospheres (1–20 % O_2, or 10 % CO_2). The sunflower seed char reached a maximum release of 55 % at 1100 °C in N_2. For wheat bran char, the molar ratio of released carbon/phosphorus was close to 2.5, which fits well with the theoretical value for carbothermic reduction of phosphates (P_2O_5(s, l) + 5C(s) → P_2(g) + 5CO(g)). At 1100 °C, in N_2, the release of phosphorus, potassium and sodium occurred mainly during the first 10 min. It was shown that $KMgPO_4$, used as a model compound, could be reduced by carbon starting from 950 °C, but that some of the phosphorus remained in the condensed phase. The work provides a better understanding of phosphorus release and presents evidence showing that carbothermic reduction reactions can be an important phosphorus release mechanism for seed- and grain-based biomass char.

1. Introduction

Phosphorus (P) is a vital element for all life as we know it. It links the building blocks of DNA together, and many metabolic pathways are dependent on molecules containing phosphorus [1]. However, in thermal conversion of biomass, the presence of phosphorus can be

Abbreviations: CP, cross polarization; CSA, chemical shift anisotropy; EDS, energy dispersive X-ray spectroscopy; ICDD, International Centre for Diffraction Data; ICP, inductively coupled plasma; MAS, magic angle spinning; NMR, nuclear magnetic resonance; OES, optical emission spectrometry; PDF, powder diffraction file; SEM, scanning electron microscopy; TGA, thermal gravimetric analysis; XRD, X-ray diffraction.

* Corresponding author.
E-mail address: haw@kt.dtu.dk (H. Wu).

https://doi.org/10.1016/j.fuel.2023.127706
Received 15 December 2022; Received in revised form 28 January 2023; Accepted 4 February 2023
Available online 11 February 2023

problematic. Some of the process-related challenges reported for phosphorus-rich biomass include slagging in burners fired with grains [2,3], and blockage of baghouse filters and severe ash deposition on economizers when combusting wheat bran in a grate-fired unit [4]. Animal biomass such as chicken litter was reported to cause agglomeration problems and wall slagging in a fluidized bed unit [5], and co-combustion using meat- and bone meal caused deactivation of selective catalytic reduction catalysts in pulverized fuel combustion [6]. Several of these problems are associated with the release of phosphorus to the gas phase. Even though numerous studies have quantified the release of phosphorus from different biomass [4,7–18], the mechanism (s) responsible for the release of phosphorus to the gas phase has not been convincingly proven. However, a few hypotheses were put forward.

1.1. Phosphorus release

Wu et al. [4] showed that the release of phosphorus from a residual bran at 1100 °C correlated well with the release of potassium in an atomic ratio close to 1, and suggested that phosphorus release proceed through vaporization of KPO_3. The potassium metaphosphate; KPO_3, has a high partial pressure compared to most other phosphates of ash-forming elements [19]. However, Lane et al. [12] performed similar investigations using three different kinds of algae, and found that the release of phosphorus did not correlate with the release of alkali, indicating phosphorus is released (also) in other forms than MPO_3(g) (M = Na or K). Hedayati et al. carried out single-pellet gasification [16] and combustion [15] of poplar, wheat straw, grass, and wheat grain residues in a macro-TGA, up to a temperature of 950 °C, and showed that the main part of the phosphorus was released during devolatilization, whereas potassium was released mainly during the char conversion stage. When the same fuels were combusted with a great excess of air in an underfed pellet burner, estimated to operate in the temperature range 1100–1250 °C, almost no phosphorus was released [9]. Chen and Wu [14] showed that the release of phosphorus in pyrolysis of rice bran varied depending on the reactor feeding strategy. Heating the rice bran slowly (10 °C/min) to 900 °C resulted in almost no phosphorus release, whereas feeding into a hot reactor resulted in a phosphorus release of 15–30 %. They hypothesized that interaction between volatiles and char enhanced the phosphorus release [14].

For non-plant based calcium-rich biomasses such as meat and bone meal, and sewage sludge, carbothermic reduction reactions of calcium phosphates were hypothesized to be responsible for the release of phosphorus at high temperatures (≥1200 °C) [6,11]. In recent work, Lidman Olsson et al. [20,21], have shown that the release of phosphorus may also proceed through carbothermic reduction reactions of sodium-, potassium-, magnesium- and calcium phosphates starting from around 850 °C. These carbothermic reduction reactions may provide a plausible phosphorus release mechanism for phosphorus from biomass.

1.2. Carbothermic reduction of phosphates

Overall, a carbothermic reduction of phosphate can be described (for the phosphorus oxide part of the phosphate) as:

$$P_2O_5(s, l) + 5C(s) \rightarrow P_2(g) + 5CO(g) \quad (R1)$$

The discovery of this kind of reaction dates back to 1669 and the German alchemist Hennig Brand's search for the philosopher's stone [22]. By heating large amount of urine, Hennig Brand thermally decomposed salts in the urine to sodium phosphate ($NaPO_3$) and carbon [22,23]. Upon further heating, the following reaction is believed to have taken place [23]:

$$4NaPO_3(s, l) + 5C(s) \rightarrow Na_4P_2O_7(s, l) + P_2(g) + 5CO(g) \quad (R2)$$

When the released phosphorus oxidize upon the contact with air, a green glow can be observed, which is what Hennig Brandt witnessed. Later, other materials, such as bone and different feedstuffs, were heated in a similar manner, showing that elemental phosphorus evolve from these materials as well [23].

Today, elemental phosphorus is produced through carbothermic reduction of phosphate rock [24]. Overall, the reactions taking place in the industrial process, utilizing phosphate rock, coal and sand, can be exemplified by [24]:

$$2Ca_5(PO_4)_3F(s) + 9SiO_2(s) + 15C(s) \rightarrow 3P_2(g) + 15CO(g) + 9CaSiO_3(s, l) + CaF_2(s, l) \quad (R3)$$

Silica sand (SiO_2) is acting as a fusing agent in the reaction, but is not a requisite for the formation of elemental phosphorus.

Beck et al. [6] suggested that, in co-combustion of meat and bone meal or sewage sludge with coal, phosphorus was released through reaction *R(3)*, and then oxidized to P_4O_{10}(g) by oxygen in the combustion air. Zhang et al. [11] also hypothesized that reaction *R(3)* caused the release of phosphorus in co-pyrolysis and co-gasification of sewage sludge with coal. However, in industrial processes, reaction *R(3)* is carried out in the temperature range 1400–1500 °C [24], and experimental evidence proving that the reaction is relevant for biomass conversion is missing. Matinde et al. [25] used mass spectrometry to qualitatively study the carbothermic reduction of phosphates in sewage sludge pyrolyzed with and without coal, and found that phosphorus was present mainly as P_2 in the gas phase above approximately 1000 °C.

For plant-based biomass, the occurrence of carbothermic reduction reactions has not been studied previously. This is likely because the carbothermic reduction of phosphates, other than calcium orthophosphates, have gained little attention and the specific reaction mechanism (s) is not well-established. However, the reduction of both Ca- and Mg-metaphosphates was shown to follow a stepwise process with the corresponding pyro- and orthophosphates forming as intermediates [26,27], which can be described by the overall reactions (R4-R6) (Me = Ca or Mg):

$$2Me(PO_3)_2(s) + 5C(s) \rightarrow Me_2P_2O_7(s) + P_2(g) + 5CO(g) \quad (R4)$$

$$3Me_2P_2O_7(s) + 5C(s) \rightarrow 2Me_3(PO_4)_2(s) + P_2(g) + 5CO(g) \quad (R5)$$

$$Me_3(PO_4)_2(s) + 5C(s) \rightarrow 3MeO(s) + P_2(g) + 5CO(g) \quad (R6)$$

Using activated carbon in a 10-fold excess, Lidman Olsson et al. [21] showed that these reactions proceed above 800–950 °C (reaction R(4)) and 950–1050 °C (reaction R(5)) for both magnesium and calcium, and > 1050 °C (reaction R(6)) for magnesium. For alkali phosphates, only a few studies are available [21,27,28]. The specific reactions taking place for alkali phosphates are unclear, but at high enough temperatures; >1100–1250 °C, much of the alkali is known also the be released to the gas phase (using a carbon/phosphorus molar ratio of 5) [28]. Using a higher carbon to phosphorus molar ratio (carbon/phosphorus = 25), Lidman Olsson et al. [21] showed that the alkali phosphates react with activated carbon, with simultaneous release of alkali, already from about 800 °C.

Biomass char and ash may contain stable mixed phosphates such as $CaKPO_4$ and/or $KMgPO_4$. However, only one study of carbothermic reduction of a mixed alkali-alkaline earth phosphates was performed of an amorphous Na-K-Mg-ultraphosphate, with a molar ratio of Na/K/Mg/P of about 1/1/5/20, suggesting that the reduction proceed in numerous steps [29].

1.3. Scope of this work

The aim of this work was to identify if carbothermic reduction of phosphates is a potential phosphorus release mechanism in thermal conversion of phosphorus-rich seed- and grain-based biomass chars. Chars produced from wheat bran and sunflower seed were used to study the phosphorus release behavior in a horizontal tube reactor. The wheat

bran was rich in phosphorus, potassium and magnesium, whereas the sunflower seed also contained considerable levels of calcium and silicon. The association of phosphorus in the biomass was characterized using SEM-EDS, XRD and solid state ^{31}P NMR. The release of ash-forming elements was determined by quantifying the composition of the char and residue using ICP-OES, and the carbon release was quantified using CO and CO_2 gas analysis. By studying the release at different temperatures, atmospheres, and holding times, evidence supporting the proposed release mechanism could be obtained. Different factors potentially affecting the release, such as mass transfer limitations, or the formation of a stable mixed phosphate were briefly investigated.

2. Materials and methods

2.1. Materials

Two types of grain- and seed-based biomasses, wheat bran and sunflower seed, were used in this work. The biomasses were used as received, and consisted mainly of flakes up to approximately 5 mm in size for the wheat bran, and pellets ground and sieved to a size range of 0.6–4 mm for the sunflower seed. The chemical composition of the used wheat bran, sunflower seed, and chars produced from the biomasses is shown in Table 1.

To study the reaction between carbon and phosphate, activated carbon and $KMgPO_4$ were used as model compounds in this work. The activated carbon (product name AquaSorb 2000), resembling the carbon in biomass char, was manufactured by Jacobi Carbons AB, Sweden, and purchased in retail, where it was sold as a filter material for beverage purification. The activated carbon has previously been used to study the reactions between carbon and phosphates [21]. $KMgPO_4$ was used to resemble a stable mixed alkali – alkaline earth phosphate, which was found in seed- and grain-based biomass ash in numerous previous studies [2,3,9,16,30,31]. $KMgPO_4$ was synthesized from K_2CO_3 (99.0 %, product number 12609) and $Mg_2P_2O_7$ (≥98 %, product number 39317), supplied by Alfa Aesar, in a similar manner as reported by Berak and Podhajska-Kazmierczak [32]. K_2CO_3 and $Mg_2P_2O_7$ were ground and mixed in a cryogenic mill by Retsch, type CryoMill, using two cycles consisting of a 60 s pre-cooling at 5 Hz and 30 s of milling at 30 Hz. The mixture was then heated in air from 25 to 1000 °C at a maximum rate of 15 °C/min, and held at 1000 °C for 2 h. The sample was then ground thoroughly in an agate mortar and heated in air from 25 to 1100 °C, where it was held for 4 h. The synthesis was confirmed successful using XRD. The powder diffraction pattern is shown in Fig. S1, in the Supplementary Material. The mixture of activated carbon and $KMgPO_4$ was prepared using a cryogenic mill, as described above. The mixture was prepared with a carbon/phosphorus atomic ratio of 25/1, resulting in a 10-fold excess of carbon as per reaction R(1). The great excess of carbon represent the composition of biomass char well, and limits the interactions between the phosphate and the sample crucible. The content of ash-forming elements in the activated carbon, and in the mixture of activated carbon and $KMgPO_4$, is shown in Table S1.

Table 1
Chemical composition of wheat bran, wheat bran char, sunflower seed, and sunflower seed char with the specified span representing estimated expanded measurement uncertainty.

	Wheat bran		Sunflower seed	
	Raw[a]	Char	Raw[a]	Char
Moisture (wt %)	14.3	–	7.6	–
Char yield (wt %)	–	20.2 ± 0.7	–	27.7 ± 0.5
C (wt%)	41.6 ± 0.7	66.1 ± 0.9	43.6 ± 1.4	59 ± 2
H (wt%)	6.2 ± 0.2	1.09 ± 0.09	5.9 ± 0.3	1.0 ± 0.1
N (wt%)	2.15 ± 0.08	2.6 ± 0.2	3.5 ± 0.8	2.2 ± 0.4
O (wt%)[b]	47	15	42	21
K (wt%)	1.15 ± 0.07	6.2 ± 0.3	1.7 ± 0.2	5.3 ± 0.3
P (wt%)	0.84 ± 0.05	5.0 ± 0.2	0.92 ± 0.07	3.0 ± 0.3
Mg (wt%)	0.313 ± 0.009	1.34 ± 0.08	0.53 ± 0.04	1.8 ± 0.1
Na (wt%)	0.064 ± 0.005	0.96 ± 0.08	0.036 ± 0.004	0.15 ± 0.01
Si (wt%)	0.22 ± 0.04	0.83 ± 0.04	0.49 ± 0.06	2.2 ± 0.1
S (wt%)	0.16 ± 0.01	<0.020	0.39 ± 0.03	0.035 ± 0.006
Cl (wt%)	0.103 ± 0.001	0.091 ± 0.005	0.14 ± 0.06	0.1117 ± 0.0004
Ca (wt%)	0.095 ± 0.006	0.42 ± 0.03	0.61 ± 0.06	2.1 ± 0.2
Fe (wt%)	0.016 ± 0.005	0.066 ± 0.008	0.115 ± 0.008	0.47 ± 0.09
Al (wt%)	0.0057 ± 0.0003	0.16 ± 0.01	0.17 ± 0.01	0.70 ± 0.08
Ti (wt%)	<0.005	<0.0125	0.0094 ± 0.0004	0.050 ± 0.003
Mn (wt%)	0.0068 ± 0.0004	0.031 ± 0.004	0.0054 ± 0.0005	0.019 ± 0.001
Zn (wt%)	0.0052 ± 0.0003	0.03 ± 0.01	0.0093 ± 0.0009	0.028 ± 0.004

[a] As received.
[b] Calculated by difference.

2.2. Experiments in horizontal tube reactor

A horizontal tube reactor, previously described in detail [20], was used to convert the biomass samples, having a mass of 5–7 g. The reactor consisted of a horizontal alumina tube with water cooled flanges. The samples were placed in an alumina boat, which was pushed into the reactor using a steel rod that extended to outside of the reactor. At the reactor inlet, a water-cooled section was mounted, from which the sample could be pushed into the reactor, or retracted upon completion of the experiments, in order to achieve a fast heating or cooling rate, respectively. The temperature was measured using a thermocouple located under the sample boat, and was measured to be within ± 10 °C of the target. The temperature in the char bed may have deviated more, especially in oxidizing conditions, but the aggressive conditions did not allow for measurement of the char bed temperature. Previous studies using a similar setup showed that the char bed temperature overshoot was acceptable for ≤ 5 % O_2 in N_2 [33]. A gas mixing panel was used to prepare the desired composition of the feed gas. The flue gas was analyzed for CO, CO_2, and O_2 using a Rosemount MLT4 gas analyzer, by Emerson Process Management GmbH & Co. OHG, utilizing infrared sensors (CO and CO_2) and a paramagnetic detector (O_2).

To avoid temperature overshoot caused by exothermic reactions between volatiles and the char and/or feed gas, the conversion of the biomass was divided into a two-step process. First, the biomass was treated using flash pyrolysis by inserting it into 800 °C, where it was held for 10 min while a gas flow of 5 L/min (20 °C, 1 atm) of N_2 was fed to the reactor, and then quenched by retracting into the reactor's cooled zone. In the second step, the produced char was exposed to different atmospheres representing pyrolysis (100 % N_2), combustion (1–20 % O_2 in N_2), or gasification (10 % CO_2 in N_2), in the temperature range 900–1100 °C. Also in this step, the samples were inserted into a hot reactor to achieve a high heating rate. The wheat bran char was exposed to all three atmospheres, whereas the sunflower seed char was converted using pyrolysis (100 % N_2) only. The samples were kept in the reactor until the CO and CO_2 concentration in the flue gas was below 20 ppm, or until a holding time of 2 h was reached, whatever came first. In a few instances, a fixed holding time was used such that if vaporization of phosphates took place, the results would still be comparable. By converting the biomass using a two-step approach, the correlation between release of phosphorus and CO + CO_2 from the char in the second step could be studied since volatiles that would otherwise have interfered were already released in the first step. Char samples, and the mixture consisting of activated carbon and $KMgPO_4$, were also heated from 25 to 1135 °C in 3 L/min (20 °C, 1 atm) N_2, at a maximum heating rate of

15 °C/min, to investigate at what temperatures CO and CO_2 starts evolving from the sample due to reactions within the char. The same methodology was previously used to study the carbothermic reduction of phosphates relevant for thermal conversion of biomass [21].

2.3. Sample and residue characterization

The elemental composition of the biomasses and produced residues were determined using ICP-OES. Digestion was performed using United States Environmental Protection Agency (US EPA) method 3052. Prior to digestion, all char and ash samples were ground thoroughly in an agate mortar and the raw biomasses were ground in a cryogenic mill using the same method as described above. A sample mass of 0.05–0.5 g (depending on the amount available) was digested in 6 mL of 65 % HNO_3, 2 mL of 30 % HCl, and 2 mL of 40 % HF. 12 mL of 10 % H_3BO_3 was used for complexation, and the sample diluted to 50 mL with Milli-Q water. The samples were diluted 5 times for analysis, and 3 injections were made. The samples were analyzed in duplicates. In a few instances, the samples were digested in 5 mL of 65 % HNO_3, 1 mL of 30 % H_2O_2 and 1 mL of 50 % HBF_4 using a microwave digestor. These samples were diluted to 100 mL using ultrapure water, and then diluted 20 times for analysis, which were performed using 5 injections and not in duplicates due to the limited amount of sample available. The content of carbon, hydrogen and nitrogen in the biomass and chars was determined using a Eurovector EuroEA3000 elemental analyzer. The samples were analyzed five times each. The biomass moisture content was determined based on the mass loss from around 5 g of biomass kept in air in a muffle furnace at 105 °C for 2 h. The chlorine content of the biomass and char was determined using ion chromatography. The extraction was performed by mixing 0.4 g of sample in 4 mL of Milli-Q water for 24 h.

Selected samples were analyzed using XRD analysis. The powder diffraction patterns were collected using a Huber G670 powder diffractometer. Samples were analyzed in the 2θ range 3 to 100°, with a step size of 0.005°, using CuKα1 radiation (λ = 1.54056 Å) for 1 h. The data were collected in transmission mode from a rotating flat plate inclined 45° relative to the primary beam. The software Crystallographica Search-Match, version 3.1.0.2, with ICDD's PDF-4 + 2022 database, was used for the evaluation.

The biomass chars were analyzed using SEM. Char particles were dispersed on double-sided carbon tape mounted on an aluminum stub. Images of the chars were obtained using a Prisma E scanning electron microscope from Thermo Scientific at 15–20 kV using the secondary electron signal. EDS was used to generate elemental distribution maps and spot compositions at 15–20 kV using the backscattered electron signal.

Solid-state ^{31}P NMR spectra were measured with a 14.1 T Bruker AVIIIHD spectrometer ($\nu(^{31}P)$ = 242.91 MHz) equipped with a 4 mm CP/MAS broadband probe (Bruker). The spectra were acquired using direct excitation with a spinning frequency of 7 kHz. 6000 scans were accumulated for each spectrum with an interscan delay of 60 s. Listed chemical shifts are reported relative to H_3PO_4 (85 % in H_2O). Spectral simulation was performed using the Topspin module SOLA. CSA parameters are reported using the Haeberlen convention.

2.4. Quantification of release

The release of ash-forming elements was determined using a mass balance calculation based on mass measurements, and the elemental composition of the sample, before and after treatment in the tube reactor. The same methodology has previously been used successfully to determine the release of ash-forming elements from biomass and model compounds [4,33,34]. The release is calculated using eq (1).

$$R_i = \left(1 - \frac{m_{residue} \cdot C_i^{residue}}{m_{sample} \cdot C_i^{sample}}\right) \cdot C_i^{sample} \quad (1)$$

where R_i (mol/kg) is the release of element *i*, $C_i^{residue}$ (mol/kg) and C_i^{sample} (mol/kg) are the concentration of element *i*, determined using ICP-OES analysis, in the residue, and the sample (char) before treatment in the reactor, respectively, and $m_{residue}$ (kg) and m_{sample} (kg) are the mass of the residue and sample, respectively. The determined elemental composition of the chars appeared to be more accurate compared to that of the raw biomasses. The content of non-volatile elements, such as Mg and Ca, in the produced residues is similar to that of the char, whereas it was less consistent with that of the raw biomass. The chars were therefore used as reference point for the release measurements. The release of carbon was calculated by integrating the CO and CO_2 concentrations measured in the flue gas.

Visual inspection and mass measurements revealed that, for all samples treated in an inert atmosphere, there was limited interaction with the alumina crucible. The samples treated in an oxidizing atmosphere were somewhat more difficult to retrieve from the crucible, which indicate that interaction between the ash and crucible had taken place to some extent. However, based on the mass of the empty crucible measured before and after the experiments, low amounts of alumina appear to have dissolved in the sample residues. Nonetheless, the result for the samples treated in an oxidizing atmosphere may be associated with a somewhat higher uncertainty.

2.5. Carbonate content and corrected carbon/phosphorus release ratio

If the release of phosphorus is caused by carbothermic reduction reactions of phosphates to elementary phosphorus, as per reaction R(1), 2.5 carbon atoms would be consumed per phosphorus atom. However, other reactions taking place in the char may also contribute to the release of CO and CO_2. These reactions include decomposition of carbonates, such as the overall reaction R(7) for alkali carbonates (M = Na, K) [35–37].

$$2M_2CO_3(s) \rightarrow 4\ M(g) + O_2(g) + 2CO_2(g) \quad (R7)$$

The formed O_2(g) and CO_2(g) may react with carbon in the char to form additional CO(g). In an attempt to quantify the amount of carbonates in the char, ash was first produced by combusting the chars at 450 °C. This process should have consumed most of the carbon in the char, except for carbonates, which are expected to remain in the sample. By converting the sample at such a low temperature, no release of ash-forming elements should take place. In a second step, the sample was introduced into an inert atmosphere at 1100 °C. The CO and CO_2 being released in this step should mainly originate from decomposing carbonates.

Another source of CO and CO_2 may be the carbothermic reduction of alkali oxides, occurring simultaneously with the carbothermic reduction of phosphates. This reaction is represented by reaction R(8):

$$M_2O(s, l) + C(s) \rightarrow 2\ M(g) + CO(g) \quad (R8)$$

It should be noted that M_2O represent the alkali oxide fraction of a phosphate, for examples in the K_2O-P_2O_5 system. Oxides of the other elements present in the wheat bran char; Mg, Ca, Si, and Al, are not expected to be prone to reduction by carbon at 1100 °C. The molar ratio of released carbon/phosphorus, corrected for decomposition of carbonates and reduction of alkalis, was calculated using eq (2).

$$R_{C/P} = \frac{R_{COx,\ char} - \left(R_{CO,\ ash} + 2 \cdot R_{CO2,\ ash}\right) - 0.5 \cdot (R_{Na} + R_K)}{R_P} \quad (2)$$

where $R_{C/P}$ (mol/mol) is the corrected molar ratio of released carbon to phosphorus, $R_{COx,\ char}$ (mol/kg char) is the total release of CO and CO_2 from the char when treated using pyrolysis, $R_{CO,\ ash}$ (mol/kg char) and $R_{CO2,\ ash}$ (mol/kg char) are the release of CO and CO_2 originating from decomposing carbonates, respectively. The term $0.5 \cdot (R_{Na} + R_K)$ represents the CO originating from reduction of carbonates according to

reaction R(8), where R_{Na} and R_K is the release of sodium and potassium, calculated as shown in section 2.4, respectively.

2.6. Expanded measurement uncertainties

Where given, the expanded measurement uncertainties were estimated using instrument and equipment characteristics, the uncertainty of the calibration gas concentrations, and the standard deviation of the elemental composition quantifications. The uncertainties were combined using the root sum of squares method. A confidence level of 95 % was used.

3. Results and discussion

3.1. Characterization of chars

The elemental composition of the produced wheat bran char and sunflower seed char is shown in Table 1. The elemental composition was used to calculate the molar distribution of the ash-forming elements (excluding carbon and oxygen), and are shown in Fig. 1. For the wheat bran char, the ash-forming elements are dominated by phosphorus, potassium, magnesium, sodium and silicon. In the sunflower seed char, the content of phosphorus and sodium is somewhat lower, but the char contains more calcium, silicon and aluminum compared to the wheat bran char. The levels of sulfur and chlorine in the raw biomass were relatively low, and in the chars, almost none is present. This is in line with previous studies of wheat bran residues [4], sunflower seed and freshwater algae [12], which reported 80–100 % sulfur release already at 500 °C [4,12], and almost complete release of chlorine at 850 °C [12].

It is difficult to determine in what form the phosphorus is present. The chars were analyzed using XRD, and the resulting powder diffraction patterns are shown in Figs. S2 and S3. In the wheat bran char, the amount of crystalline material was almost undetectable. This is in line with previous work in which char produced from wheat grain residues were analyzed using XRD [16]. The char constitutes a major fraction of the amorphous material. However, the absence of crystalline phases also indicates that the ash-forming elements may form a mixture with a low melting temperature. In the sunflower seed char, a few crystalline phases could be identified, but in rather low quantities. These crystalline phases include $KAlSi_2O_6$ (leucite), SiO_2 (quartz) and $KMgPO_4$. The sunflower seed char contains more silicon and aluminum compared to the wheat bran char, so it is reasonable that these phases are detected in the sunflower seed char, but not in the wheat bran char. The mixed phosphate, $KMgPO_4$, detected in the sunflower seed char, has a high melting temperature [32], and was reported to be present in the ashes of thermally converted grain- or seed based biomasses in numerous previous work [2,3,9,16,30,31].

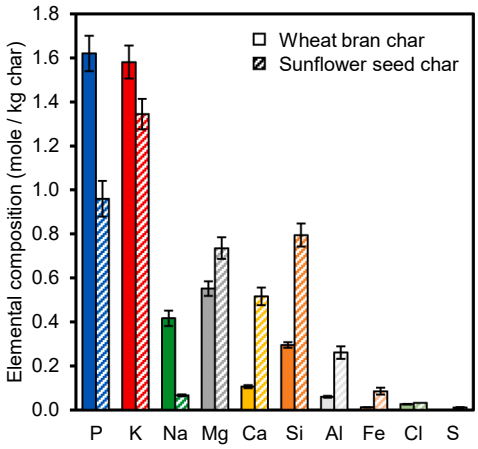

Fig. 1. Molar distribution of ash-forming elements (excluding oxygen) in wheat bran char and sunflower seed char produced through flash pyrolysis in N_2 at 800 °C using a holding time of 10 min.

Previous studies have shown that organic phosphorus present in biomass decompose to inorganic phosphates below 350 °C [38–40]. In the wheat bran char used in this work, the inorganic phosphates may be present as alkali or alkaline earth metals, or combinations thereof. Furthermore, these phosphates may be present as meta- (PO_3^-), pyro- ($P_2O_7^{4-}$), and/or orthophosphates (PO_4^{3-}). Because the reactivity towards carbothermic reduction reactions can be quite different depending on the type of phosphate, additional characterization of the chars was conducted using SEM-EDS and solid-state ^{31}P NMR.

SEM images of the produced wheat bran char and sunflower seed char are shown in Fig. 2. For the wheat bran char, the image shows several smaller compartments. Some of these compartments contain units that are rich in potassium, magnesium and phosphorus. Similar units have been observed by others in wheat grain residues [4,15], and are likely what is left of globoids after the flash pyrolysis. Globoids are inclusions rich in phytate, an organic phosphate acting as a phosphorus and energy storage in many plant-based biomasses [41,42]. Having several phosphate groups, phytate also acts as a storage molecule for cations such as potassium and magnesium [41,42]. Phytate decomposes to inorganic phosphates and char above around 400 °C [20]. Despite the relatively high content of sodium in the wheat bran char, low concentrations of sodium were detected in the mapping of the globoid residues. This indicates that sodium may be present in other forms, such as sodium carbonate.

Similar compartments were not found in sunflower seed char, but areas rich in phosphorus, potassium, and magnesium were found. From the EDS-mapping in Fig. 2, it can be seen that phosphorus and potassium appear in the same areas. Magnesium appears in some of these areas, but seems to be somewhat more evenly distributed across the char structure.

To semi-quantitatively assess how phosphorus may be associated in the chars, the ratio of cationic charge/phosphorus atom in each of the pixels in the EDS-maps were calculated and compiled in relative distribution functions, shown in Fig. 2. The frequency was scaled proportionally to the amount of phosphorus in each pixel. The contribution of each cation to the cationic charge/phosphorus atom ratio is also shown in Fig. 2. For wheat bran char, the cationic charge/phosphorus atom ratio is centered close to 2, which resembles the ratio in pyrophosphates. For the sunflower seed char, the distribution is centered closer to 3, which resembles the ratio in orthophosphates. Interestingly, this difference is not apparent from the overall composition of the SEM-EDS maps, shown in Table 2, which shows a similar ratio for both chars. From Fig. 2, it can also be seen that the contribution from magnesium to the ratio is highest around a ratio of 3, whereas the contribution by calcium is fairly low. This indicates that most of the phosphorus may be associated as K-Mg-phosphates, and less as Ca-phosphates. The overall content of calcium is higher in the sunflower seed char, compared to the wheat bran char (based on the ICP-OES results). However, from the SEM-EDS analysis, about the same amount of calcium seem to be associated with phosphorus in the two chars. This confirms that calcium is present in other forms, such as calcium carbonate, in the sunflower seed char.

Solid state ^{31}P NMR analysis was performed to investigate in what form phosphorus may be bonded to potassium and magnesium in the chars. Solid state ^{31}P NMR spectra of the wheat bran char and sunflower seed char are shown in Fig. 3. For both samples, all peaks are located within the range 0 ± 10 ppm, but with a broad peak extending to about −20 ppm for the wheat bran char. The spectra for the wheat bran char is less distinct compared to the sunflower seed char. However, many of the same peaks appear to be present in both samples.

A number of literature references for meta-, pyro-, and orthophosphates of sodium, potassium, calcium and magnesium are included in Fig. 3. The literature data show that, generally, the phosphate peaks appear in the order meta-, pyro-, and orthophosphate when going from

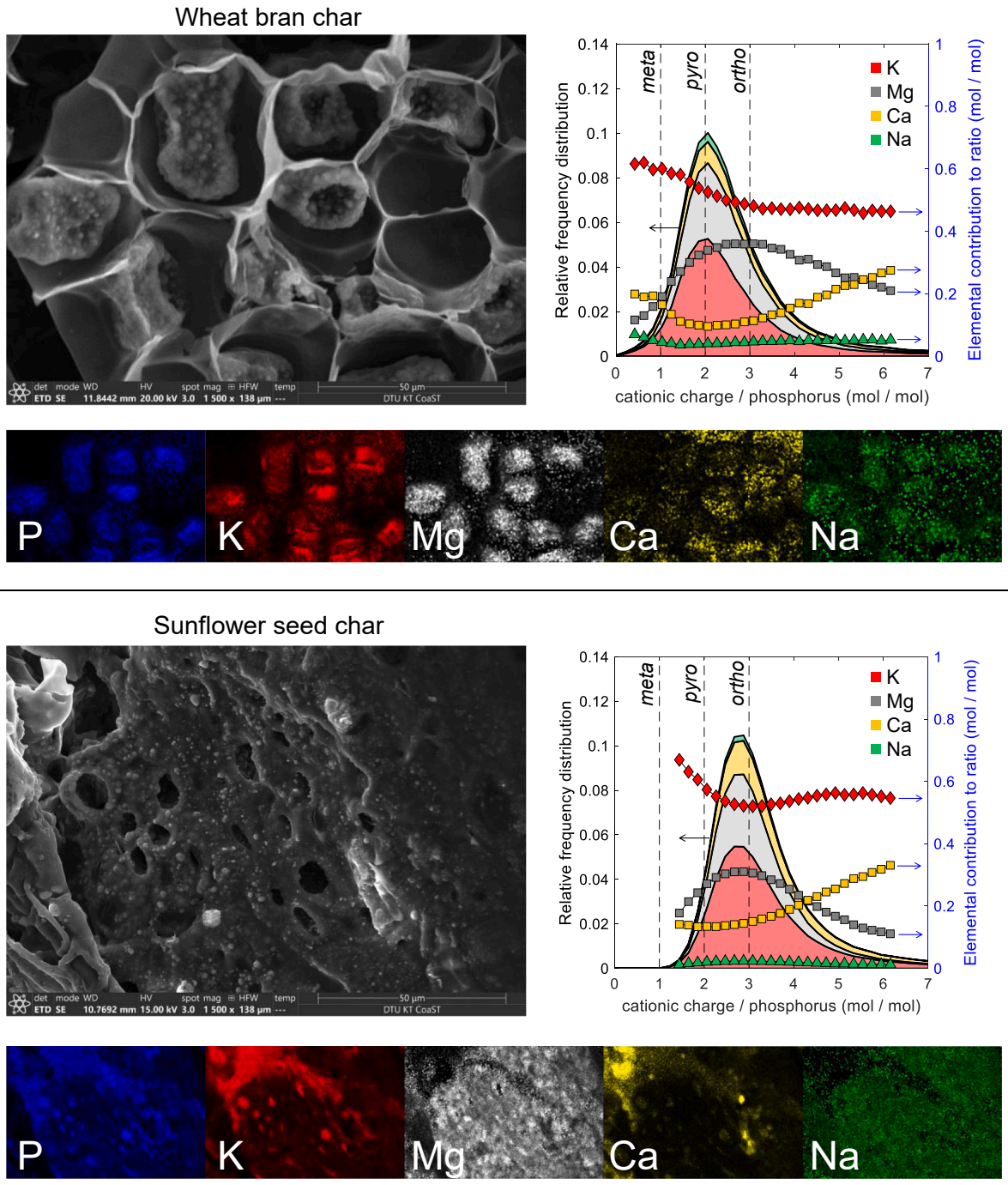

Fig. 2. SEM images of wheat bran char (upper) and sunflower seed char (lower) produced in N_2 at 800 °C using a holding time of 10 min, with EDS mapping showing the major ash-forming elements (excluding carbon and oxygen). The intensity of the EDS maps are scaled individually to show the location of each element and does not represent concentration relative to other elements. Note that almost no sodium was detected for the sunflower seed char, but it has been included here for consistency. The molar ratio of cationic charge/phosphorus atom was calculated for each of the pixels in the EDS-maps and are shown in graphs as relative frequency distributions scaled proportionally using the content of phosphorus in each pixel. Symbols (right axis) represent the contribution of each cation to the cationic charge/phosphorus atom ratio. The cationic charge/phosphorus atom ratio in meta-, pyro-, and orthophosphates are shown using vertical dashed lines.

Table 2
Overall composition in atom% (on a carbon and oxygen free basis) of wheat bran char and sunflower seed char in SEM images shown in Fig. 2, determined using EDS.

	P	K	Na	Mg	Ca
Wheat bran char	35	41	3	19	3
Sunflower seed char	37	43	0	16	4

low to high chemical shift. None of the two spectra have peaks at chemical shifts typical for metaphosphates (<-10 ppm), which is in line with the SEM-EDS results. However, both chars exhibit peaks in the pyrophosphate region, and to some extent also the orthophosphate region. Considering that magnesium was found together with potassium and magnesium (SEM-EDS), it is likely that the phosphate in the char samples are present in the form of ortho- or pyrophosphates consisting of both potassium and magnesium.

A deconvolution was performed to identify the individual peaks in

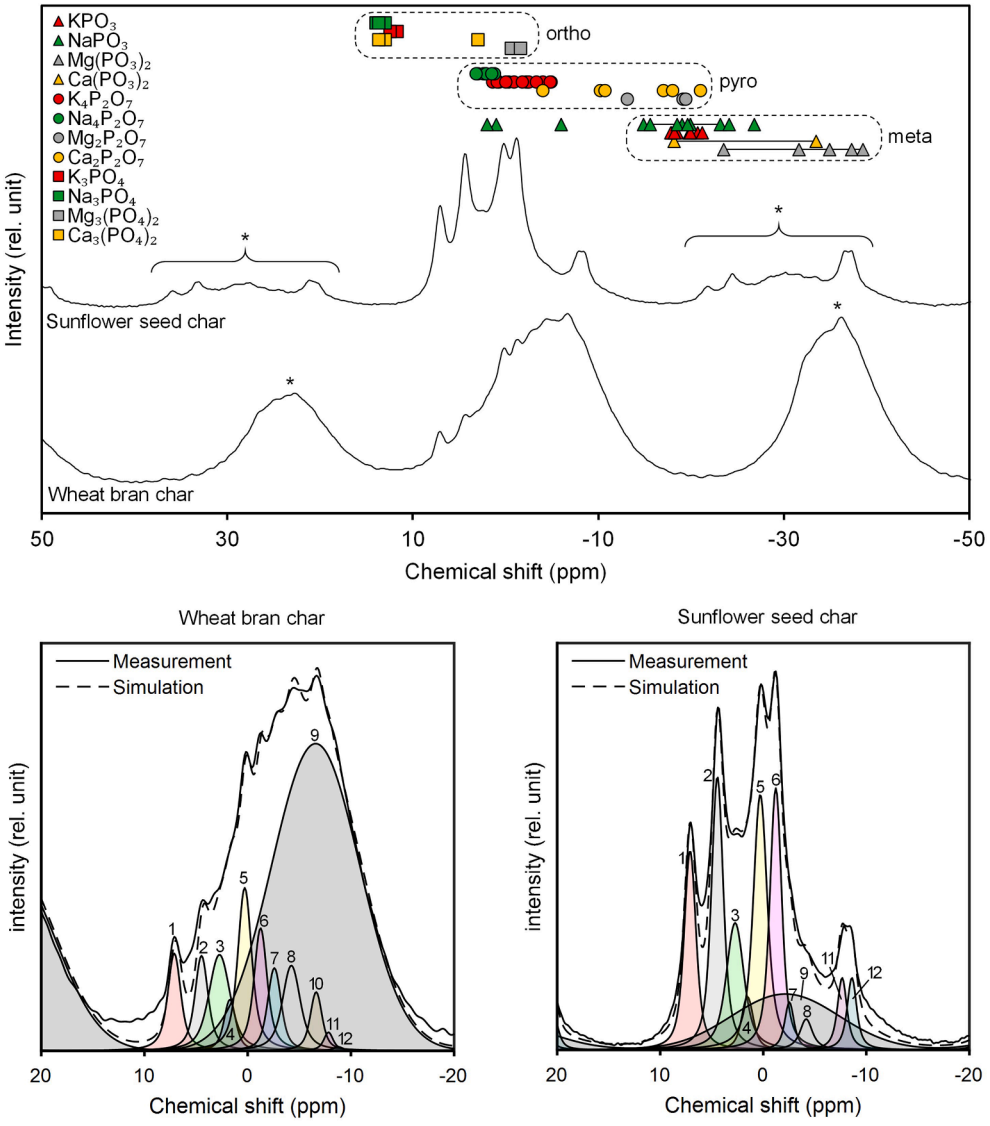

Fig. 3. Solid-state ^{31}P NMR spectra of wheat bran char and sunflower seed char together with literature data for meta-, pyro-, and orthophosphates of sodium, potassium, magnesium, and calcium (upper), with expanded plots of the isotropic peaks for wheat bran char (lower left), and sunflower seed (lower right) showing the spectral simulation. '*' marks spinning side bands. The horizontal lines in the literature data represent broad peaks present for glasses of metaphosphates. The reference data were obtained from [43–52].

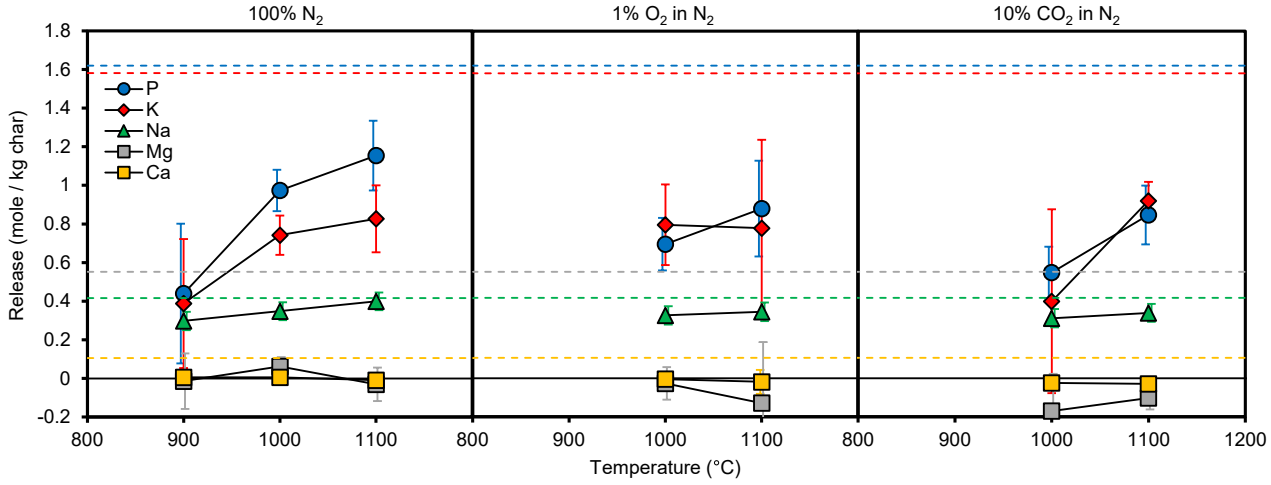

Fig. 4. Release of ash-forming elements from wheat bran char at different temperatures in N_2 (left), 1 % O_2 in N_2 (middle), and 10 % CO_2 in N_2 (right). The dashed colored horizontal lines represent the content of each element in the char, i.e. the maximum possible release. The holding time was 2 h, except for the samples treated at 1000 and 1100 °C in N_2, which had a holding time of 1 h because little conversion was taking place (CO + CO_2 concentration in flue gas was < 20 ppm).

the spectra. The resulting peaks are shown in the expanded plots of Fig. 3, and the isotropic chemical shift of the individual peaks are shown in Table S2, together with the relative intensity and asymmetry parameter. For both chars, peak number 9 accounts for most of the phosphorus. However, for the wheat bran char, it accounts for about 80 % of the phosphorus, whereas it for the sunflower seed makes up around 30 %. Peak 9 is very broad, and the asymmetry parameter, η, is higher compared to the other peaks, which indicates the peak may represent amorphous phosphates. It is plausible that peak 9 represents amorphous K-Mg-pyrophosphate, which based on the XRD, ICP-OES and SEM-EDS results, is expected to be present to a larger extent in the wheat bran char. Additional work on mixed alkali – alkaline earth phosphates is required before peaks accurately can be assigned to the different types of phosphates.

3.2. Release of ash-forming elements at different conditions

The release of the major ash-forming elements in the wheat bran char at different temperatures and in different atmospheres is shown in Fig. 4. The release of phosphorus increase from 27 % (of the total phosphorus) at 900 °C to 71 % at 1100 °C in a N_2 atmosphere. In the oxidizing atmospheres (1 % O_2 in N_2 and 10 % CO_2 in N_2), the release of phosphorus is about 20 % lower compared to the inert atmosphere. This observation supports that carbothermic reduction reactions might be an important release mechanism, especially under inert or reducing conditions. The consumption of carbon in the oxidizing atmospheres leaves less carbon available for reactions with phosphates, which may explain the lower release of phosphorus.

All calcium and magnesium is expected to remain in the sample residues, but both elements have been included in Fig. 4, because they provide a good indication of whether the mass balance is met. For both calcium and magnesium, the mass balance is satisfactorily met in all cases. Considerable amounts of alkali is also released from the wheat bran char. Whereas most of the sodium is released in the temperature range 900–1100 °C, the release of potassium instead seems to follow that of phosphorus to a greater extent. However, the atmosphere seems to have a smaller effect on the release of alkali, suggesting that different mechanisms may govern the release of alkali compared to phosphorus.

It should also be stressed that the samples exposed to 1000 and 1100 °C in an inert environment was held in the reactor for a shorter duration (1 h) since little conversion (based on CO + CO_2 release) was taking place, compared to the oxidizing atmospheres in which the experiments were stopped after 2 h. If vaporization of alkali phosphates is important, a longer holding time would be expected to have resulted in a higher release, which was not the case.

The release of phosphorus, alkali, and alkaline earth metals from sunflower seed char in an inert atmosphere is shown in Fig. 5. Generally, the release of phosphorus and potassium from sunflower seed char is lower compared to that of the wheat bran char. The release of phosphorus is in the range of 10–20 % (of the total phosphorus) in the temperature range 900–1000 °C, and increase to 55 % at 1100 °C. Three possible explanations for the lower release of phosphorus from sunflower seed char is that:

1) A larger fraction of phosphorus is associated as orthophosphates, compared to in the wheat bran char, in which the phosphorus seem to be associated mainly as pyrophosphate. Orthophosphates are generally less reactive in carbothermic reduction reactions compared to pyrophosphates, which may explain the lower release of phosphorus [21].
2) Some of the phosphorus may interact with calcium, which is present in higher quantities in the sunflower seed char, and be retained in the residues. Calcium orthophosphate ($Ca_3(PO_4)_2$) is less reactive compared to magnesium orthophosphate ($Mg_3(PO_4)_2$) towards carbothermic reduction reactions [21].

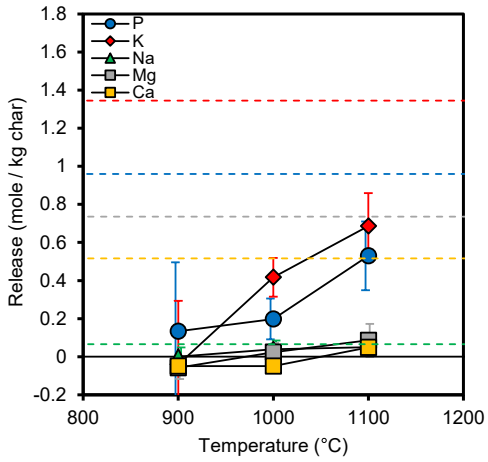

Fig. 5. Release of ash-forming elements from sunflower seed char at different temperatures in N_2. The dashed colored horizontal lines represent the content of each element in the char, i.e. the maximum possible release. The holding time was 2 h for the samples treated at 900 and 1000 °C, and 1 h for the sample treated at 1100 °C.

3) Some of the phosphorus may be present in the form of phosphosilicate(s), which may be less prone to undergo carbothermic reduction reactions. Even though the SEM-EDS analysis showed that the concentration of silicon in the phosphorus-rich areas was low, it cannot be excluded that some parts of the sunflower seed char contained areas rich in both phosphorus and silicon.

3.3. Molar ratio of released potassium to phosphorus

The most volatile alkali phosphates (relevant for biomass conversion) are the metaphosphates (MPO_3, M = Na, K), whereas the pyro- and orthophosphates have lower vapor pressures and are not expected to vaporize in the investigated temperature range [19]. The metaphosphates vaporize congruently [19]:

$$MPO_3(l) \rightarrow MPO_3(g) \quad \text{(R9)}$$

Which means that the molar ratio of released potassium/phosphorus should be close to 1 if alkali metaphosphate vaporization is the dominating release mechanism. Since the level of potassium is higher compared to sodium in both the wheat bran char and sunflower seed char, and since the SEM-EDS analysis showed that phosphorus is primarily present in the same areas as potassium, it is reasonable to expect that mainly KPO_3 vaporization would take place. It should also be noted that the vapor pressure of KPO_3 is higher compared to $NaPO_3$ [19]. The molar ratio of released potassium/phosphorus was therefore calculated and is shown in Fig. 6. In the inert environment, the molar ratio of released potassium/phosphorus is around 0.7–0.8 for the wheat bran char. For the sunflower seed char, the molar ratio is about 0.5 at a temperature of 1000 °C, and increase to 0.8 at 1100 °C. Based on these results, phosphorus may not be released in the form of KPO_3(g), at least not only in this form. Generally, the ratio appears to be somewhat higher in the oxidizing atmospheres (1 % O_2 or 10 % CO_2 in N_2), but the higher measurement uncertainty in the oxidizing atmospheres makes it difficult to draw specific conclusions about differences compared to the inert atmosphere.

The release of alkali may be caused by carbothermic reduction of alkali phosphates. An example of such a reaction is represented by reaction (R10) (M = K, Na) [21,28]:

$$MPO_3(l) + 3C(s) \rightarrow M(g) + \tfrac{1}{2}P_2(g) + 3CO(g) \quad \text{(R10)}$$

However, the release of alkali is possibly also caused by the thermal decomposition of sodium- and/or potassium carbonates (reaction R(7)).

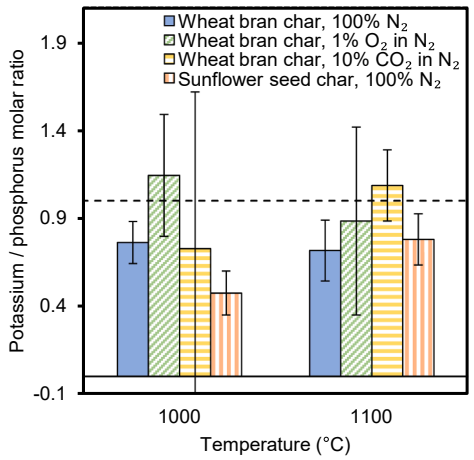

Fig. 6. Molar ratio of released potassium/phosphorus from wheat bran char and sunflower seed char at different temperatures and atmospheres. The higher uncertainties in the oxidizing atmospheres are probably a consequence of the rather small ash residues left after the experiment, which were partly melted and more difficult to collect from the crucible.

The wheat bran char contained some sodium, but only minor amounts of sodium was present in the phosphorus-rich areas based on SEM-EDS. Because no sulfates or chlorides are present in the char, based on ICP-OES, it is likely that the sodium is associated as Na-carbonate. This is also in line with the measured release of sodium. Almost all sodium was released over the temperature range 900–1100 °C, whereas the release of potassium appear to follow that of phosphorus closer (Fig. 4). In the sunflower seed char, which contained considerable amounts of calcium, carbonates may be present in the form of calcium carbonate.

3.4. Molar ratio of released carbon to phosphorus

The molar ratio of released carbon/phosphorus, corrected for the amount of carbon originating from decomposing carbonates and reduction of released alkali, is shown in Fig. 7. For wheat bran char, the calculated molar ratio is close to 2.5, which suggests that carbothermic reduction reactions may take place. Because of the high measurement uncertainty of the values obtained for sunflower seed char at 900 and 1000 °C, these results are left out. As can be seen in Fig. 7, the result obtained at 1100 °C is also associated with considerable uncertainty. However, the measured value is higher compared to that of the wheat bran char. Possible explanations for the higher value of the sunflower seed char are:

1) Other species than oxides of phosphorus and alkali may be reduced at 1100 °C. However, iron oxides are the only other oxides in the sunflower seed char that are expected to undergo reduction at this temperature. The content of iron in the sunflower seed char is comparatively low.
2) Some of the released phosphorus and alkali may be captured by other species in the char. This would make the molar ratio of carbon to phosphorus appear higher compared to if no capture took place. The sunflower seed char contains less phosphorus compared to the wheat bran char, but the levels of magnesium, calcium, silicon, and aluminum are higher. If these ash-forming elements can capture gaseous phosphorus, this may explain the difference between sunflower seed char and wheat bran char in Fig. 7.

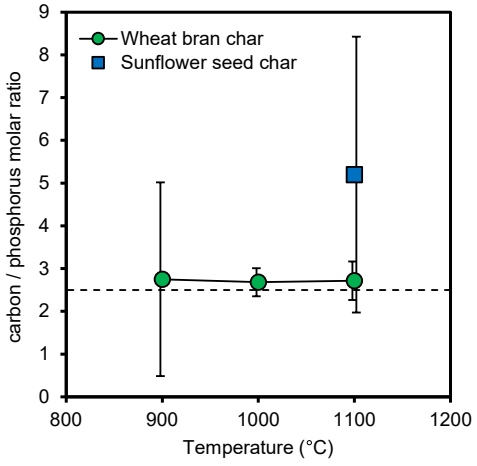

Fig. 7. Molar ratio of released carbon/phosphorus in an inert environment for wheat bran char and sunflower seed char. The release of carbon is corrected for the CO and CO_2 originating from decomposition of carbonates, and the reduction of alkali oxides. The horizontal dashed line at 2.5 represent the ratio corresponding to carbothermic reduction of phosphate.

3.5. Effect of oxygen concentration on the release of ash-forming elements

To investigate how an increasingly oxidizing environment effects the release of ash-forming elements, the wheat bran char was converted at 1100 °C using different O_2 concentrations (0, 1, 5, 10, or 20 %) in the feed gas. The release of ash-forming elements from the wheat bran char is shown in Fig. 8. The release of both phosphorus and potassium decrease with increasing oxygen concentration. The release of phosphorus decrease to about one third of the release taking place in an inert environment. A plausible explanation is that oxygen is consuming carbon in the char, leaving less carbon available to participate in carbothermic reduction reactions. In an oxidizing atmosphere, the ash layer forming on the char surface, might also capture some of the phosphorus released from lower parts of the char bed. The oxygen diffusing inwards in the ash layer, may oxidize the released phosphorus diffusing outwards, resulting in the formation of phosphorus oxides that may be more prone to form condensed species with other ash-forming elements in the ash layer.

Considering that carbon should be more prone to react with an oxidizer such as O_2(g), compared to condensed phosphates, it can be debated whether carbothermic reduction reactions are actually contributing to the phosphorus release in strongly oxidizing environments (e.g. 20 % O_2 in N_2), or whether the release is mainly caused by vaporization of phosphates at these conditions. However, it should be

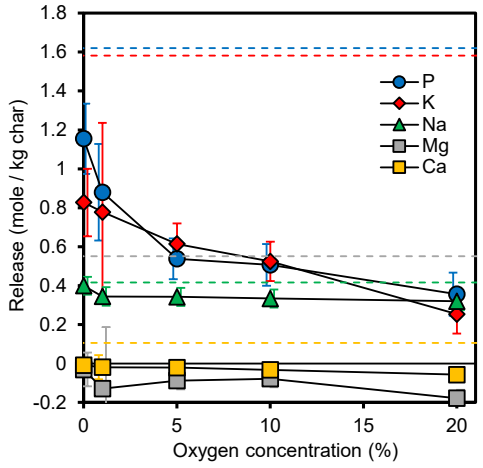

Fig. 8. Release of ash-forming elements from wheat bran char at 1100 °C in N_2 as a function of oxygen concentration in the feed gas. The content of each element in the char is marked with horizontal dashed lines.

noted that the current system is a fixed bed, in which combustion of the char takes about 10 min (at 20 % O_2, 1100 °C). Hence, carbothermic reduction reactions can still proceed in the lower parts of the char bed that are not immediately exposed to O_2(g), and may therefore account for some of the release observed in the oxidizing environments.

Considering that the release of potassium is quite similar to that of phosphorus, it is likely that the carbothermic reduction reaction involves a reduction of K-(Mg)-phosphates, resulting in a simultaneous release of potassium and phosphorus. If vaporization of KPO_3 was the dominating release mechanism, it may also be argued that the release should be less dependent on atmosphere. This is clearly not the case for wheat bran char.

Interestingly, the release of sodium remains unchanged with the feed gas oxygen concentration. This confirms that sodium is present in other forms, for example as sodium carbonate. The decomposition of sodium carbonate may be less dependent on the carbon content in the char, and thereby also the feed gas oxygen concentration.

3.6. Release rate

The rate of release of the different ash-forming elements in the wheat bran char was studied at 1100 °C, by keeping samples in the reactor using different holding times. The result of these tests are shown in Fig. 9. It is clear that most of the release of sodium, potassium and phosphorus takes place within the first ten minutes. Almost all sodium is released, whereas the release of potassium and phosphorus appear to level out at about 50 and 70 %, respectively.

The release of phosphorus from wheat bran residues [4] and algae [12] was previously quantified using setups similar to the setup used in this work. In combustion of wheat bran residues [4], the release of phosphorus was reported to be about 70 % at 1100 °C [4], which is higher compared to the results in this work (Fig. 8). For algae, the release of phosphorus was in the range of 40–70 % (depending on the type of algae) at 1100 °C, and in contrast to this work, reported to be independent on whether the algae was converted using pyrolysis, gasification, or combustion [12]. However, in both studies [4,12], the samples were exposed to a N_2 atmosphere for 15–60 min prior to exposing the samples to oxidizing conditions. Since most of the release takes place within the first ten minutes (Fig. 9), the results reported in previous studies [4,12] may actually better represent the release in pyrolysis conditions, rather than combustion or gasification.

The molar ratio of released carbon/phosphorus and potassium/phosphorus throughout the process is shown in Fig. 10. Initially, the

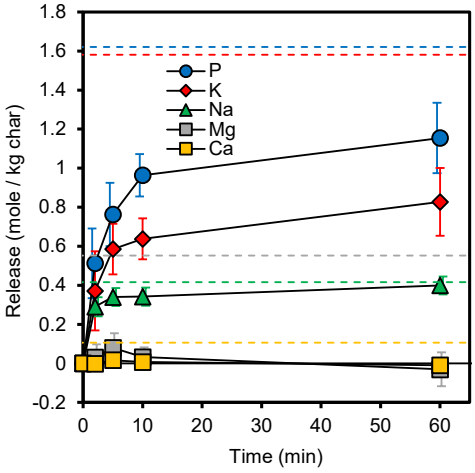

Fig. 9. Release of ash-forming elements from wheat bran char at 1100 °C in N_2 as a function of time. The content of each element in the char is marked with horizontal dashed lines.

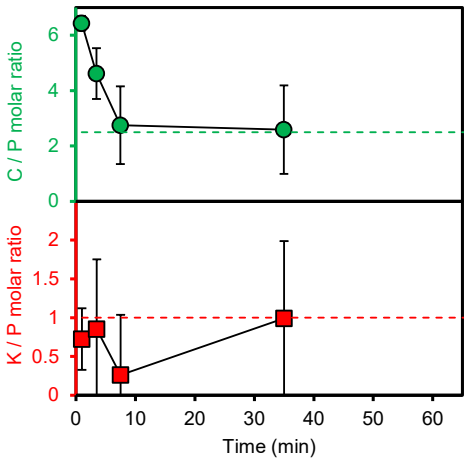

Fig. 10. Molar ratio of released carbon/phosphorus (upper) and potassium/phosphorus (lower) from wheat bran char converted in N_2 at 1100 °C as a function of time. The molar ratio at each specific time was calculated as an average of each adjacent point (shown in Fig. 9). The horizontal dashed lines indicate the value expected for carbothermic reduction reactions of phosphate (C/P = 2.5) and for KPO_3 vaporization (K/P = 1).

released molar ratio of carbon/phosphorus is above 6, but during the first 5–10 min it falls to about 2.5, where it seem to stabilize. A molar ratio of 2.5 correspond well to the theoretical amount required for the carbothermic reduction of phosphate as per reaction R(1). The initial high value may be due to decomposing carbonates contributing to the carbon release.

The potassium/phosphorus molar ratio was generally close to, or below one throughout the process. However, the uncertainty of the potassium/phosphorus molar ratio has a large span and it is not possible to elucidate if the molar ratio change throughout the process.

The reason phosphorus release is leveling out at about 70 % remains to be explored. Some possible reasons for this phenomenon are listed below:

1) If phosphorus is released through a carbothermic reduction reaction, local mass transfer limitations may inhibit the release. The phosphorus-rich areas of the wheat bran char observed using SEM-EDS may become depleted in carbon as the reaction proceed.
2) The remaining phosphorus may be present as stable phosphates, having a low vapor pressure, or a low reactivity with respect to carbothermic reduction reactions. Lidman Olsson et al. [21] have previously shown that, among the alkali (Na and K), and alkaline earth (Mg and Ca) meta-, pyro- and orthophosphates, under similar conditions, only Ca orthophosphate is stable enough not to participate in carbothermic reduction reactions to any great extent at 1100 °C. But the amount of calcium in the wheat bran char is too low to form stable phosphates with all the remaining phosphorus. However, certain mixed phosphates, such as $KMgPO_4$, are stable (judging by the melting temperature) and may therefore also exhibit a low reactivity in carbothermic reduction reactions.
3) Other phosphorus species may form in the char that are stable under these specific conditions. Such species may possibly be phosphites or phosphides. These may form simultaneously with, or as side reactions to, the carbothermic reduction reactions [53]. Perhaps, they may also form upon reactions between released elemental phosphorus and solid/liquid species present in the char [54]. Such reactions have been shown to take place between CaO(s) and P_2(g), resulting in formation of phosphide (Ca_3P_2) and phosphite ($Ca_3(PO_3)_2$). Little is known about such species, especially for the alkali phosphides/phosphites.

3.7. Effect of mass transfer limitations

For the char samples treated in N_2 at 1100 °C, much of the carbon remained in the residues, which visually also appeared to maintain its structure. However, to investigate if local depletion of carbon and mass transfer limitations may cause the phosphorus release to level out (point 1 in the previous section), a wheat bran char sample held at 1100 °C for 1 h in N_2, was ground thoroughly in an agate mortar to a fine powder and reintroduced into the reactor for an additional 1 h. The effect of mixing on the release of ash-forming elements, is shown in Fig. 11. Some additional phosphorus and potassium appear to have been released after mixing and a second thermal treatment at 1100 °C in N_2, but considering the expanded measurement uncertainties, no firm conclusion can be drawn.

During the second exposure to 1100 °C, more carbon was released, corresponding to roughly 25 % of the carbon released during the first exposure to 1100 °C. Even though there seem not to be a considerable additional release of phosphorus, the release of carbon indicates that mass transfer limitations in the char may limit carbothermic reduction reactions within the char. However, it cannot be excluded that oxygen and/or moisture was adsorbed on the char during the grinding process, and then reacted with carbon during the second exposure to 1100 °C, thereby resulting in the release of CO and CO_2. Another possibility is that stable phosphites and/or phosphides, formed during the first exposure to 1100 °C, oxidized to phosphates in the presence of air during the grinding process and then reacted with carbon upon re-exposure to 1100 °C.

3.8. Carbothermic reduction of $KMgPO_4$

$KMgPO_4$, which has a melting temperature of 1520 °C [32], is generally considered to be a stable phosphate. To investigate if $KMgPO_4$ is reduced by carbon to any great extent at 1100 °C, or if its presence may explain why some phosphorus is not released (point 2 in section 3.6), it was heated in a mixture with activated carbon (10-fold stoichiometric excess of carbon as per reaction R(1)) from 25 to 1135 °C. The release of phosphorus, potassium, magnesium, and oxygen, is summarized in Table 3. The carbon evolving from the mixture (as CO + CO_2) is shown in Fig. 12. Both phosphorus and potassium are released in considerable quantities. However, at 1135 °C, when the experiment is completed, little CO and CO_2 is evolving from the sample, which suggests that stable compounds may have formed. Considering that most of the oxygen was released as CO or CO_2, the remaining compounds must be reduced species, perhaps phosphites or phosphides, such as Mg_3P_2

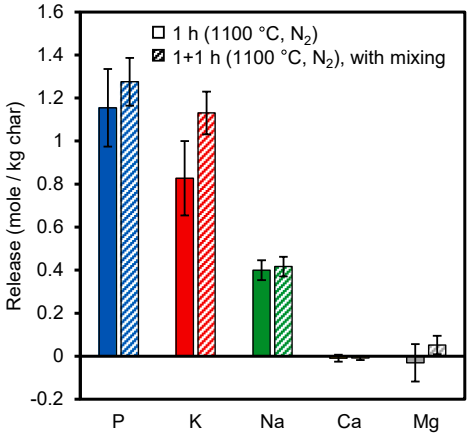

Fig. 11. Release of ash-forming elements from wheat bran char at 1100 °C in N_2 using a holding time of 1 h, without additional treatment (filled columns) and after thorough grinding in an agate mortar and a second pyrolysis treatment at 1100 °C in N_2 using a holding time of 1 h (striped columns).

Table 3
Release of elements from the model compound $KMgPO_4$ when heated with activated carbon in a 10-fold stoichiometric excess from 25 to 1135 °C in N_2.

	P [a]	K [a]	Mg [a]	O [b]
Release (%)	69 ± 5	44 ± 5	4 ± 3	81 ± 4

[a]Determined using ICP-OES.
[b]Determined using CO and CO_2 gas analysis.

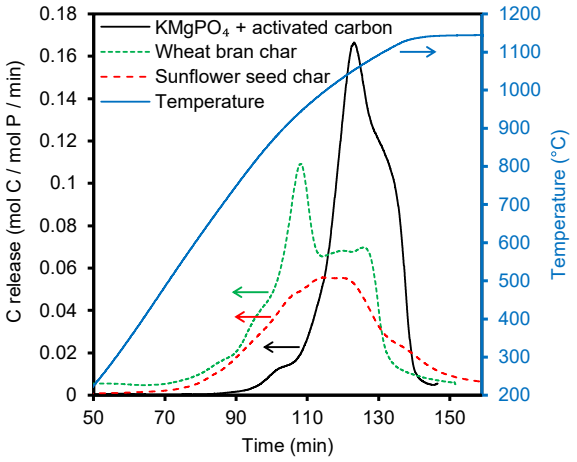

Fig. 12. Carbon release rate, calculated using CO + CO_2 concentration in fluegas and scaled using the molar amount of phosphorus in the original sample, (left axis) and temperature (right axis) when heating wheat bran char, sunflower seed char, or $KMgPO_4$ mixed with activated carbon, from 25 to 1135 °C in 3 L/min N_2.

[53]. Based on these results, the formation of stable phosphorus species in the biomass chars provides a plausible explanation for why not all phosphorus is released.

For comparison, the release of carbon from wheat bran char and sunflower seed char heated in the same manner is also shown in Fig. 12. The biomass chars are releasing a somewhat lower amount of carbon and the release is shifted towards somewhat lower temperatures. The lower amount of carbon released from the biomass chars may be a consequence of mass transfer limitations in the chars. The somewhat different profiles may also indicate that 1) $KMgPO_4$ is not representative for phosphates in the biomass char, 2) the carbon in the biomass char is more reactive, and/or 3) carbonates may be present in the biomass char, which upon decomposition are contributing to the carbon release at lower temperature.

3.9. Comparison with reduction of model compounds

As seen in the previous section, wheat bran char and sunflower seed char release CO and CO_2 at a lower temperature compared to when the model compound $KMgPO_4$ is reduced using activated carbon. However, the characterization of wheat bran char indicated that phosphorus is present mainly in the form of pyrophosphates. Few studies have investigated the carbothermic reduction of potassium and magnesium phosphates, especially pyrophosphates. However, Lidman Olsson et al. [21] recently recorded the CO and CO_2 evolution from different phosphates mixed with activated carbon when heated in an inert atmosphere from 20 to 1135 °C. Whether CO and CO_2 profiles for model compounds can be used to predict the evolution of CO and CO_2 from phosphorus-rich biomass was investigated by comparing the results in this work with those of Lidman Olsson et al. [21]. A simulated CO and CO_2 profile for the wheat bran char and sunflower seed char was calculated using the results for individual phosphates in Lidman Olsson et al. [21] using eq

(3):

$$\dot{n}_{COx,char}(t) = \sum n_{COx,j}(t)x_j \quad (3)$$

where $\dot{n}_{COx,\,char}(t)$ represents the release rate of CO and CO_2 from the biomass char relative to the amount of phosphorus in the sample (mol carbon/mol phosphorus/s) at time t (s), $\dot{n}_{COx,\,j}(t)$ is the release rate of CO and CO_2 from the model phosphate j (mol carbon/mol phosphorus/s), and x_j represents the mole fraction of phosphorus assumed to be present as phosphate j in the calculation.

For wheat bran char, the simulated value was calculated by assuming that phosphorus is present as pyro- and metaphosphates in a ratio that fulfills the cationic charge to phosphorus ratio of 1.8 (corresponding to the molar ratio of (K + 2 Mg + 2Ca)/P obtained using ICP-OES, with Na excluded because the observations in this work suggests sodium is present mainly in other forms than phosphates). The relative distribution of potassium and magnesium between meta- and pyrophosphates was assumed to be equal:

$$\frac{x_{KPO3}}{x_{K4P2O7}} = \frac{x_{Mg(PO3)2}}{x_{Mg2P2O7}} = \frac{x_{Ca(PO3)2}}{x_{Ca2P2O7}} \quad (4)$$

A comparison between the simulated and experimental CO and CO_2 profile for wheat bran char is shown in Fig. 13. For wheat bran char, the calculated CO and CO_2 profile agrees quite well with the experimental results. This indicates that phosphates in biomass char participate in carbothermic reduction reactions similarly to what was observed for individual model phosphates.

4. Conclusions

The release of phosphorus, potassium, and sodium, from wheat bran char and sunflower seed char at different temperatures was quantified. The effect of different atmospheres on the release was investigated using wheat bran char. It can be concluded that carbothermic reduction reactions can be important for the release of phosphorus from biomass char, especially under inert and reducing conditions, based on the following observations:

- The release of phosphorus was higher in an inert environment compared to the oxidizing environments. The consumption of carbon in the oxidizing environments may limit the extent of carbothermic reduction reactions.
- At 1100 °C, the molar ratio of released carbon/phosphorus approached 2.5 for the wheat bran char, which corresponds well to the theoretically expected value for reduction of phosphates.
- SEM-EDS and ^{31}P NMR analysis showed that phosphorus is likely associated mainly as K-Mg-pyrophosphates in wheat bran char, whereas a larger extent of orthophosphates appear to be present in the sunflower seed char. The former are more reactive in carbothermic reduction reactions, which may explain the difference in phosphorus release from the two different chars.
- The phosphate $KMgPO_4$, which is often found in seed-and grain-based biomass residues from thermal conversion of biomass and generally considered a stable phosphate, undergoes carbothermic reduction in the temperature range used.

It should be stressed that the release of phosphorus may be strongly dependent on the conversion technology applied. For example, in fluidized bed combustion, in which the biomass may be converted rapidly, and the temperature generally is lower, less phosphorus may be released compared to in grate-fired units, in which char consumption is slow and parts of the bed may locally experience reducing conditions. The extent of gas–solid interactions may also influence the overall release because bed material or ash-forming elements in the condensed phase perhaps may recapture some of the gaseous phosphorus species.

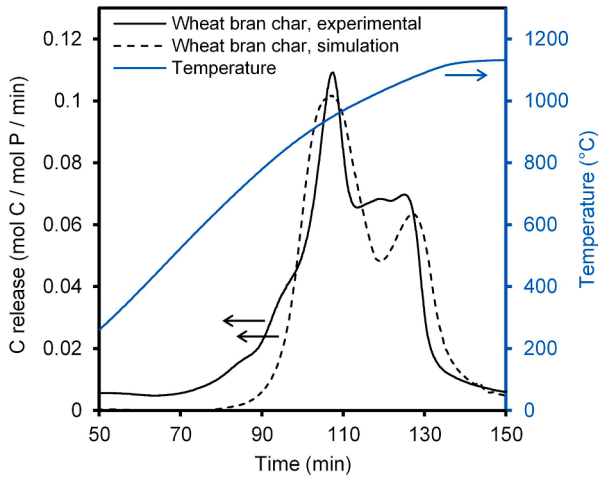

Fig. 13. Evolution of CO and CO_2 from wheat bran char when heated in N_2 from 25 to 1135 °C, together with a CO and CO_2 profile calculated using the results from Lidman Olsson et al. [21].

CRediT authorship contribution statement

Emil O. Lidman Olsson: Conceptualization, Methodology, Validation, Formal analysis, Investigation, Writing – original draft, Writing – review & editing, Visualization. **Daniel Schmid:** Formal analysis, Investigation, Writing – review & editing. **Oskar Karlström:** Resources, Writing – review & editing, Funding acquisition. **Kasper Enemark-Rasmussen:** Formal analysis, Investigation, Resources, Writing – review & editing. **Henrik Leion:** Writing – review & editing, Supervision. **Songgeng Li:** Supervision. **Peter Glarborg:** Conceptualization, Methodology, Resources, Writing – review & editing, Supervision. **Kim Dam-Johansen:** Resources, Supervision. **Hao Wu:** Conceptualization, Methodology, Resources, Writing – review & editing, Supervision, Project administration, Funding acquisition.

Declaration of Competing Interest

The authors declare that they have no known competing financial interests or personal relationships that could have appeared to influence the work reported in this paper.

Data availability

Data will be made available on request.

Acknowledgements

The project has received financial support from the Sino-Danish Center for Education and Research, from Technical University of Denmark, from the Academy of Finland (project: Chemical challenges in gasification of biomass and waste, 355914 and 353318), and from Nordic Energy Research (project: NEST - Nordic Network in Solid Fuels towards Future Energy Systems, 120626). Great appreciation goes to Anne Juul Damø for helping with the SEM-EDS analysis of some of the samples.

Appendix A. Supplementary data

Supplementary data to this article can be found online at https://doi.org/10.1016/j.fuel.2023.127706.

References

[1] Westheimer FH. Why nature chose phosphates. Science 1987;235:1173–8. https://doi.org/10.1126/science.2434996.

[2] Lindström E, Sandström M, Boström D, Öhman M. Slagging characteristics during combustion of cereal grains rich in phosphorus. Energy Fuels 2007;21:710–7. https://doi.org/10.1021/ef060429x.

[3] Eriksson G, Grimm A, Skoglund N, Boström D, Öhman M. Combustion and fuel characterisation of wheat distillers dried grain with solubles (DDGS) and possible combustion applications. Fuel 2012;102:208–20. https://doi.org/10.1016/j.fuel.2012.05.019.

[4] Wu H, Castro M, Jensen PA, Frandsen FJ, Glarborg P, Dam-Johansen K, et al. Release and transformation of inorganic elements in combustion of a high-phosphorus fuel. Energy Fuels 2011;25(7):2874–86.

[5] Billen P, Creemers B, Costa J, Van Caneghem J, Vandecasteele C. Coating and melt induced agglomeration in a poultry litter fired fluidized bed combustor. Biomass Bioenergy 2014;69:71–9. https://doi.org/10.1016/j.biombioe.2014.07.013.

[6] Beck J, Brandenstein J, Unterberger S, Hein KRG. Effects of sewage sludge and meat and bone meal Co-combustion on SCR catalysts. Appl Catal B Environ 2004;49:15–25. https://doi.org/10.1016/j.apcatb.2003.11.007.

[7] Liu WJ, Zeng FX, Jiang H, Yu HQ. Total recovery of nitrogen and phosphorus from three wetland plants by fast pyrolysis technology. Bioresour Technol 2011;102:3471–9. https://doi.org/10.1016/j.biortech.2010.10.135.

[8] Hannl TK, Häggström G, Hedayati A, Skoglund N, Kuba M, Öhman M. Ash transformation during single-pellet gasification of sewage sludge and mixtures with agricultural residues with a focus on phosphorus. Fuel Process Technol 2022;227:107102. https://doi.org/10.1016/j.fuproc.2021.107102.

[9] Hedayati A, Falk J, Borén E, Lindgren R, Skoglund N, Boman C, et al. Ash Transformation during Fixed-Bed Combustion of Agricultural Biomass with a Focus on Potassium and Phosphorus. Energy Fuels 2022;36(7):3640–53.

[10] Xiao Y, Zhao R, Chen J. Fixation of phosphorus in ash during cocombustion of sewage sludge and coals: influence of coal and steam. Energy Fuels 2022;36:4396–403. https://doi.org/10.1021/acs.energyfuels.2c00053.

[11] Zhang Q, Liu H, Li W, Xu J, Liang Q. Behavior of phosphorus during Co-gasification of Sewage Sludge and Coal. Energy Fuels 2012;26:2830–6. https://doi.org/10.1021/ef300006d.

[12] Lane DJ, van Eyk PJ, Ashman PJ, Kwong CW, de Nys R, Roberts DA, et al. Release of Cl, S, P, K, and Na during thermal conversion of algal biomass. Energy Fuels 2015;29(4):2542–54.

[13] Liaw SB, Wu H. High-phosphorus fuel combustion: effect of oxyfuel conditions on PM_{10} emission from homo- and heterogeneous phases. Energy Fuels 2017;31:2317–23. https://doi.org/10.1021/acs.energyfuels.6b02337.

[14] Chen X, Wu H. Transformation and release of phosphorus during rice bran pyrolysis: effect of reactor configurations under various conditions. Fuel 2019;255:1–7. https://doi.org/10.1016/j.fuel.2019.115755.

[15] Hedayati A, Lindgren R, Skoglund N, Boman C, Kienzl N, Öhman M. Ash transformation during single-pellet combustion of agricultural biomass with a focus on potassium and phosphorus. Energy Fuels 2021;35:1449–64. https://doi.org/10.1021/acs.energyfuels.0c03324.

[16] Hedayati A, Sefidari H, Boman C, Skoglund N, Kienzl N, Öhman M. Ash transformation during single-pellet gasification of agricultural biomass with focus on potassium and phosphorus. Fuel Process Technol 2021;217:1–12. https://doi.org/10.1016/j.fuproc.2021.106805.

[17] Hedayati A, Lestander TA, Rudolfsson M, Thyrel M, Öhman M. Fate of phosphorus and potassium in single-pellet thermal conversion of forest residues with a focus on the char composition. Biomass Bioenergy 2021;150:1–12. https://doi.org/10.1016/j.biombioe.2021.106124.

[18] Häggström G, Hannl TK, Hedayati A, Kuba M, Skoglund N, Öhman M. Single pellet combustion of sewage sludge and agricultural residues with a focus on phosphorus. Energy Fuels 2021;35:10009–22. https://doi.org/10.1021/acs.energyfuels.1c00882.

[19] Lopatin SI. Vaporization in phosphate systems. Russ J Gen Chem 1997;67:193–211.

[20] Lidman Olsson EO, Glarborg P, Leion H, Dam-Johansen K, Wu H. Release of P from pyrolysis, combustion, and gasification of biomass—A model compound study. Energy Fuels 2021;35:15817–30. https://doi.org/10.1021/acs.energyfuels.1c02397.

[21] Lidman Olsson EO, Glarborg P, Leion H, Dam-Johansen K, Wu H. An exploratory study of phosphorus release from biomass by carbothermic reduction reactions. Proc Combust Inst 2022.

[22] Emsley J. The Sordid Tale of Murder, Fire, and Phosphorus. The 13th element. New York: John Wiley & Sons, Inc.; 2000.

[23] Gleason W. An introduction to phosphorus: history, production, and application. JOM 2007;59:17–9. https://doi.org/10.1007/s11837-007-0071-y.

[24] Diskowski H, Hofmann T. Phosphorus. Ullmann's Encycl Ind Chem 2000:725–46. https://doi.org/10.1002/14356007.A19_505.

[25] Matinde E, Sasaki Y, Hino M. Phosphorus gasification from sewage sludge during carbothermic reduction. ISIJ Int 2008;48(7):912–7.

[26] Yamamoto K-I, Kato A, Seiyama T. Reduction of Calcium Phosphates with Carbon (In Japanese). J Soc Chem Ind Japan 1968;71(3):367–72.

[27] Kalmykov SI, Shevchenko NP, Dyankova YN. About the Properties of Ultraphosphates of Alkali and Alkaline Earth Metals. Message XV. Investigation of the Reduction of Ultraphosphates of Sodium, Potassium, Magnesium with Carbon (In Russian). Izv Akad Nauk Kazachskoj SSR Ser Chim 1985;1:7–14.

[28] Shevchenko NP, Ulanova NM. Kinetics and Mechanism of Carbon Redoing of $(MPO_3)_n$ Sodium and Potassium Phosphates (in Russian). Zhurnal Neorg Khimii 1989;34:1704–9.

[29] Shevchenko NP, Ulanova NM, Kozhevnikova VP, Zhuravlev GN. Reduction of Amorphous Ternary Sodium-Potassium-Magnesium Ultraphosphate by Carbon. J Appl Chem Ussr 1990;63:6–10.

[30] Boström D, Eriksson G, Boman C, Öhman M. Ash transformations in fluidized-bed combustion of rapeseed meal. Energy Fuels 2009;23:2700–6. https://doi.org/10.1021/ef800965b.

[31] Grimm A, Skoglund N, Boström D, Öhman M. Bed agglomeration characteristics in fluidized quartz bed combustion of phosphorus-rich biomass fuels. Energy Fuels 2011;25:937–47. https://doi.org/10.1021/ef101451e.

[32] Berak J, Podhajska-Kaźmierczak T. Phase equilibria in the ternary system MgO-K_2O-P_2O_5. Part I. The partial system MgO-$Mg_3(PO_4)_2$–K_3PO_4. Pol J Chem 1991;65:1137–49.

[33] van Lith SC, Alonso-Ramírez V, Jensen PA, Frandsen FJ, Glarborg P. Release to the gas phase of inorganic elements during wood combustion. Part 1: Development and evaluation of quantification methods. Energy Fuels 2006;20:964–78. https://doi.org/10.1021/ef050131r.

[34] Frandsen FJ, van Lith SC, Korbee R, Yrjas P, Backman R, Obernberger I, et al. Quantification of the release of inorganic elements from biofuels. Fuel Process Technol 2007;88(11-12):1118–28.

[35] Motzfeldt K. The thermal decomposition of sodium carbonate by the effusion method. J Phys Chem 1955;59:139–47. https://doi.org/10.1021/j150524a011.

[36] Kim JW, Lee HG. Thermal and carbothermic decomposition of Na_2CO_3 and Li_2CO_3. Metall Mater Trans B Process Metall Mater Process Sci 2001;32:17–24. https://doi.org/10.1007/s11663-001-0003-0.

[37] Sergeev D, Yazhenskikh E, Kobertz D, Müller M. Vaporization behavior of Na_2CO_3 and K_2CO_3. Calphad Comput Coupling Phase Diagrams Thermochem 2019;65:42–9. https://doi.org/10.1016/j.calphad.2019.02.004.

[38] Uchimiya M, Hiradate S. Pyrolysis temperature-dependent changes in dissolved phosphorus speciation of plant and manure biochars. J Agric Food Chem 2014;62:1802–9. https://doi.org/10.1021/jf4053385.

[39] Uchimiya M, Hiradate S, Antal MJ. Dissolved phosphorus speciation of flash carbonization, slow pyrolysis, and fast pyrolysis biochars. ACS Sustain Chem Eng 2015;3(7):1642–9.

[40] Xu G, Zhang Y, Shao H, Sun J. Pyrolysis temperature affects phosphorus transformation in biochar: chemical fractionation and ^{31}P NMR analysis. Sci Total Environ 2016;569–570:65–72. https://doi.org/10.1016/j.scitotenv.2016.06.081.

[41] Lott JNA, Ockenden I, Raboy V, Batten GD. Phytic acid and phosphorus in crop seeds and fruits: a global estimate. Seed Sci Res 2000;10:11–33. https://doi.org/10.1017/s0960258500000039.

[42] Phytic FAW, Acid., Chem.. Plant phosphorus compd. 1st ed.,. Waltham, USA: Elsevier; 2013. p. 75–134.

[43] Grimmer AR, Haubenreisser U. High-field static and MAS ^{31}P NMR: Chemical shift tensors of polycrystalline potassium phosphates $P_2O_5{\cdot}xK_2O$ ($0 \leq x \leq 3$). Chem Phys Lett 1983;99:487–90. https://doi.org/10.1016/0009-2614(83)80180-8.

[44] Duncan TM, Douglas DC. On the ^{31}P chemical shift anisotropy in condensed phosphates. Chem Phys 1984;87:339–49. https://doi.org/10.1016/0301-0104(84)85115-0.

[45] Hayashi S, Hayamizu K. High-resolution solid-state ^{31}P NMR of alkali phosphates. Bull Chem Soc Jpn 1989;62:3061–8. https://doi.org/10.1246/bcsj.62.3061.

[46] Prabhakar S, Rao KJ, Rao CNR. A magic-angle spinning ^{31}P NMR investigation of crystalline and glassy inorganic phosphates. Chem Phys Lett 1987;139:96–102. https://doi.org/10.1016/0009-2614(87)80158-6.

[47] Brow RK, Phifer CC, Turner GL, Kirkpatrick RJ. Cation effects on ^{31}P MAS NMR chemical shifts of metaphosphate glasses. J Am Ceram Soc 1991;74(6):1287–90.

[48] Cheetham AK, Clayden NJ, Dobson CM, Jakemana RJB. Correlations between ^{31}P N.M.R. Chemical shifts and structural parameters in crystalline inorganic phosphates. J Chem Soc, Chem Commun 1986:195–7.

[49] Mudrakovskii IL, Shmachkova VP, Kotsarenko NS, Mastikhin VM. ^{31}P nmr study of I-IV group polycrystalline phosphates. J Phys Chem Solids 1986;47:335–9. https://doi.org/10.1016/0022-3697(86)90022-3.

[50] Kohler SJ, Ellett JD, Klein MP. ^{31}P NMR chemical shielding tensors of α-$Ca_2P_2O_7$. J Chem Phys 1976;64(11):4451–8.

[51] Turner GL, Smith KA, Kirkpatrick RJ, Oldfieldt E. Structure and cation effects on phosphorus-31 NMR chemical shifts and chemical-shift anisotropies of orthophosphates. J Magn Reson 1986;70(3):408–15.

[52] Jäger C, Ehrt D. Investigations of solid state reactions of binary polyphosphate - Fluoride systems by means of thermal analysis, x-ray diffraction and NMR spectroscopy: III. System $Mg(PO_3)_2 + MgF_2$. Z Phys Chem 1988;159:103–12. https://doi.org/10.1524/zpch.1988.159.Part_1.103.

[53] Schlesinger ME. The thermodynamic properties of phosphorus and solid binary phosphides. Chem Rev 2002;102:4267–301. https://doi.org/10.1021/cr000039m.

[54] Vesolovskii ZP, Kriklivyi DI, Klimovich AI. Interaction of elemental phosphorus with calcium oxide (In Russian). Chim Prom 1976:34–5.